

Design of Model Predictive Control and IoT for Experimental Dual Axis Solar Tracker System based on FPGA

Elsayed A. M. BaBars

Department of Mechanical Engineering
Faculty of Engineering, Sinai University - Arish Campus
Arish, North Sinai, Egypt
elsayedbabars@gmail.com

Saber M. Abdraboo

Department of Mechanical Engineering
Faculty of Engineering at Shoubra, Benha University
Cairo 13511, Egypt
saberabdraboo@yahoo.com

Shady Y. El-Mashad

Department of Computer Systems Engineering
Faculty of Engineering at Shoubra, Benha University
Cairo 13511, Egypt
shady.elmashad@feng.bu.edu.eg

Mohamed El-sayed M. Essa

Department of Electrical Power and Machines Engineering
Institute of Aviation Engineering and Technology, Egyptian
Aviation Academy Imbaba Airport
Giza 12815, Egypt
mohamed.essa@iaet.edu.eg

Abstract— In this paper, the experimental design and investigation of a dual-axis sensor-based solar tracking system (DASTS) for a 300 W PV system is carried out based on a field programmable gate array (FPGA) as the heart of the system. A model predictive control (MPC) approach is proposed for precise control of the experimental DASTS system. Moreover, classical proportional integral and derivative (PID) and fractional order PID (FOPID) control methods were proposed in order to make a fair comparison with MPC and demonstrate the efficiency and distinctive performance of the proposed controller. Based on the practical numerical and graphical results of the performance of the different methods in DASTS, it was found that the MPC outperforms the other methods, as it showed a significant increase in the generation efficiency by 20.2% compared to the fixed solar system. A modern approach was also presented, which exploits the FPGA, which supports Internet of Things (IoT) technology, to improve the performance of solar energy tracking, by monitoring the system's measurements and thus increasing the efficiency of power generation from the system. Applying the capabilities of IoT technology allows remote monitoring and control of DASTS, which helps in making the right decisions based on sensor readings. Ultimately, based on the experimental system's results, it is evident how well the suggested system performs in terms of improving energy harvesting efficiency when compared to fixed panels. It also increases the generated energy by 20.2% by utilizing MPC and IoT technology.

Keywords— Solar Tracker; FPGA; VHDL; MATLAB; PID; FOPID; MPC; Dual Axis Tracker.

I. INTRODUCTION

Due to the pressing need to transition to clean and sustainable energy in order to protect the environment, using new and renewable sources to generate electricity has become a significant problem on a

global scale. As a result, one of the most important goals of many countries is to reach zero emissions by 2050 [1].

The utilization of renewable energy in electricity generation is increasing dramatically, and the most important of these sources are geothermal energy, wind energy, solar energy and biomass. This increase in use is supported by reducing the cost of production and policies that help the transition to low-carbon energy sources. In addition, the application of renewable energy in main energy is expected to rise from a value of 5% in 2018 to about value in 2050 around 45% [2]. As the global renewable energy size reached 2537 GW in the finish of 2019, a growth of 176 GW from 2018 [3].

Solar energy and wind energy are among the sources that dominate the growth in the use of renewable energy, and this is estimated at about 90% of the amount of newly added renewable energy in the world, which is naturally supported by the continuous reduction in development costs. Because of the Covid -19 pandemic, the spread of renewable energy has been affected and hindered, despite the continuous and clear increase in the use of renewable energy [4, 5]. From [1–5], it is evident that renewable energy is still being utilized constantly and in increasing quantities. Among the most important pioneering countries in this field is China, which has a clear footprint in this effort, and it performs effectively in the global scene for the use of renewable energy and the spread of exploitation of solar and wind energy systems [6]. As a result, China occupied an important position that made it one of the biggest installers of solar energy schemes [7].

This is a result of the steadily declining installation costs and advancements in solar energy technology. Furthermore, most nations in the world—led by the United States—have recently

shown a steady rise in the installed capacity of solar energy. [8]. As a result, as solar photovoltaic energy systems are manufactured more and more efficiently, energy can be saved safely and cleanly by using fewer fossil fuels and a greater amount of renewable energy sources, which will also improve sustainable development by lowering carbon emissions. [9]. There are many different variables on which electrical power generation through photovoltaic systems depends [10, 11], including but not limited to module characteristics, environmental conditions, and module orientation. It is known that changing environmental conditions directly affect the amount of production generated from photovoltaic energy.

As a result, many studies have focused on overcoming this problem and increasing generation efficiency by integrating supplementary apparatuses like maximum power point tracking systems (MPPTS), cooling systems and solar tracking structures [13]. We find that the process of generating photovoltaic energy depends greatly on the solar radiation falling through sunlight, as well as the directions of the photovoltaic units facing the seasonal and diurnal movements of the Earth [14, 15]. Therefore, the largest production capacity of the system is in the case of perpendicular sunlight falling on the surface of the photovoltaic units. Usually, to achieve this purpose, photovoltaic modules are installed with ideal and specific direction angle values for elevation and azimuth angles as described in [16]. This is named an immovable flat panel system. Though immovable flat panel systems generate electrical power during their facility life, the generation of power is much less than their capacity. Based on this context, the efficiency of fixed systems is considered low amount of generation in comparing with other systems.

The tracking systems of solar have grown research concern to increase PV power production and have been planned in latest literature. The tracking systems of solar can be categorized into two leading systems established on number of degrees of freedom: tracking schemes based on single-axis and tracking schemes based on dual-axis [17, 18]. In addition, the types of tracking systems are allocated into two sorts depending on the control method: closed-loop and open-loop control systems [19]. Therefore, there are many existing literature studies that revolve around tracking systems of solar founded on their driving approaches, as described in [20, 21], which contain both sensor-based and tracking based on sensor-less systems.

The reason for China's leadership is due to the continuous progress in solar energy technology and the clear decrease in the cost of installing and maintaining these systems. In addition, one of the most important countries interested in this field, which over time has been interested in increasing the installed capacity of solar energy, is the US [8]. As a result, improving the production and manufacturing of solar photovoltaic systems can increase the guarantee of energy supply by decreasing the utilization of fossil fuels and growing the usage of renewable energy sources, which will lead to a reduction in carbon emissions [9].

In the fixed flat panel systems, the modules of PV are ranged by means of predetermined best angle values for direction as explained in [16], i.e. azimuth and elevation angles. In these systems, the energy production is much less than its capacity, and thus the efficiency of these systems is relatively low, although these systems generate electrical energy throughout their service life. To solve this problem, attention has been paid to moving the solar panels with the movement of the sun, as is the case in solar tracking systems. Therefore, solar tracking systems occupied an important research position for many researchers and were proposed in recent literature to increase PV power generation. As discussed the tracking is categorized based on the number of degrees of freedom: uniaxial and biaxial solar tracking systems [17, 18]. In addition, each type of tracking system can be classified into two kinds based on the control method: closed-loop and open-loop control [19]. Solar tracking systems have been studied based on their driving methods, as discussed in [20, 21], including sensor-less based tracking systems.

Recent researches have concentrated on the improvement of solar systems based sensor-less depending on open-loop control for single-axis solar configurations [22]. The tracker system was mathematically developed by introducing a tracking procedure algorithms based on the geometric of sun-earth relationships and the forecasting for radiation of solar. In the same way, authors in [23] demonstrated an open-loop control based on a schedule of tracking. The schedule of tracking is developed based on data collection for conditions of weather and astronomical estimations for the position of sun (azimuth angle) in the sky, be dependent on date and time. The study exposed that the tracker with schedule attained via calculations of astronomical is superior to tracker with photo resistor with value about 4.2%, mainly on cloudy days.

In [24], The discussion focuses on rational models of solar tracking, taking into consideration the position of the sun and the equations governing its movement in astronomy. The research introduced a recommendation for methods of iterative numerical to maintain the trackers with high accuracy. Besides, an optimal backtracking approach is proposed by authors in [25] to avoid the formation of shadows on tracking systems with dual-axis movement. The amount of generated energy by the system with this tracking technique was found that 1.31% higher than amount of PV based on astronomical tracking.

The authors in [26] utilized the T2FSMC for tracking one-axis solar systems, taking into consideration the light intensity as it plays a crucial role in calculating the efficiency estimation. Conversely, the creation of the most illustrative factor in T2FSMC is a must to acquire significant effects such as recommended firefly-algorithm as given in [27]. In [28], The implemented solar tracker resulted in a 46% increase in total power. The article in [29] suggests MPC that is used to control the tracker based on dual axis movement via MATLAB toolbox.

The proposed work is concerned with taking full advantage of the capabilities of MPC controllers to control the field of solar trackers. To achieve this goal, there are two important design elements in an MPC application that must be carefully taken into consideration, namely the designed design system and the embedded hardware device. Recently, there are more

commercially offered embedded hardware bases for field industrial controllers, including Digital Signal Processing (DSP), Advanced RISC Device (ARM), FPGA, and Application Specific Integrated Circuits (ASIC). One of the hardware options is the FPGA, which stands out due to its notable advantages, including its exceptional flexibility and superior computing efficiency. FPGA-devices have a numerous programmable logic resources which could be exploited directly in order to implement many complex computations in the hardware. In addition, recent increasing progress in the technical aspect makes it easier to integrate FPGAs with related peripherals and microprocessors to develop a complete efficient embedded system. It is characterized by guaranteeing the functionality of the entire system that is implemented as well as assisting in the improvement of the accuracy and flexibility of the system design, which can lead to a large reduction in the number of design cycles [30]. Moreover, with the versatility of the implemented architecture including features such as parallel computing and pipelines, it helps FPGAs achieve much better processing speed of various software implementations [31]. As a result, it makes FPGAs particularly attractive and focused for computationally intensive tasks.

Recently, there has been a significant focus and emphasis on the implementation of MPC controllers on FPGA devices. A comprehensive study has been done, giving good guidelines for using FPGAs in industrial control, and this is given in [32]. We find that the authors in [33] proposed exploiting the coprocessor to increase the speed of the basic part of executing calculations in a sequential manner. The interior point approach is used for online optimization in a MATLAB/Handel-C co-design solution that has been suggested for the quick prototyping of an MPC application on an FPGA device, as detailed in [34-35]. A comparison of the active group method with the internal point strategy was made by applying it to an FPGA chip using the Handel-C procedure, and it became clear through this comparison that the active group strategy is more efficient in finding solutions to small-space problems [36]. A comprehensive explanation of MPC and the active group method in development and improvement theory was presented in [37]. In addition, a general discussion of the details of FPGA-based MPC algorithm for different servo motor tracking control systems has been made in [37]. Recent study has examined the integration of Internet of Things (IoT) with Field-Programmable Gate Array (FPGA)-based systems control in solar tracking applications. The aim is to improve performance by implementing advanced control approaches [38- 39]. This research emphasizes the potential of integrating FPGA with IoT connectivity to achieve greater sustainability and efficiency in solar energy [40]. The Internet of Things (IoT) enables capabilities such as data analysis, real-time monitoring, and remote control [41- 42]. Systems of solar tracking can be optimized for upgraded performance and efficiency of generation energy [41- 42]. In this paper, through exploiting FPGA's parallel processing capabilities, the control system achieves real-time responsiveness and efficient resource utilization crucial for dynamic solar tracking applications. Advanced control algorithms including PID, FOPID, and MPC are implemented and evaluated to enhance tracking accuracy and adaptability, offering trade-offs between precision, stability,

and response time. The integration of a Xilinx Spartan-7 based Edge Acceleration board further enhances computational power for complex control algorithms and data processing tasks, ensuring efficient resource utilization and high reliability.

II. SYSTEM DESCRIPTION

It is very well known that the common PV models are categorized into two models of PV. The two models are utilized to simulate the behavior of a PV system based on several diodes. The two types are called single and double diodes for the PV model. The model of the single diode is considered the simplified PV model. As a result, it is used to model the PV system in this paper. It has four main components parallel diode to source, source of photocurrents, shunt resistance (R_{sh}), and internal resistance of PV (R_{pv}). [13, 15, 19-23].

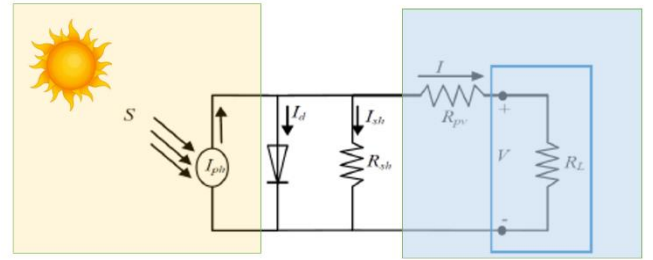


Fig. 1. Single-diode PV circuit [10]

The load current can be calculated according to Kircho's law as the incoming current from the process photocurrents I_{ph} minus the diode current I_d and the shunt current I_{sh} as follows:

$$I = I_{ph} - I_d - I_{sh} \quad (1)$$

The output current from the module and the basic equation that describes the characteristics of the strong current of the solar panel (I) and the voltage of the solar panel (V) are given in the following equation:

$$I = I_{ph} - I_0 \left(e^{\frac{V_d}{V_T}} - 1 \right) - \left(\frac{V + R_{pv}I}{R_{sh}} \right) \quad (2)$$

$$V_d = V + I R_{pv} \quad (3)$$

$$V_T = \frac{n K T}{q} \quad (4)$$

Where: I_0 stands for the saturation diode current, I_d is diode current strength, K is Boltzmann constant = $1.38 * 10^{23}$ J / K, N is the material parameter of PV, q is the movement of electron= $1.602 * 10^{19}$, R_{sh} is shunt resistance, T is temperature, V_d is diode voltage, and V_T is temperature voltage [22].

The simplification of the above equation becomes the following equation:

$$I = I_{sc} \left[1 - c_1 \left(e^{\frac{V - \Delta V}{c_2 V_{oc}}} - 1 \right) \right] + \Delta I \quad (5)$$

$$c_1 = \left(1 - \frac{I_m}{I_{sc}} \right) e^{\frac{-V_m}{c_2 V_{oc}}} \quad (6)$$

$$c_2 = \frac{V_m - 1}{\ln \left(1 - \frac{I_m}{I_{sc}} \right)} \quad (7)$$

$$\Delta I = I_{ph} - I_{sc} \quad (8)$$

$$I_{ph} = \frac{S}{S_{ref}} (I_{sc} + K_1 \Delta I) \quad (9)$$

$$\Delta V = R_{pv} \Delta I - K_v \Delta T \quad (10)$$

$$\Delta T = T - T_{ref} \quad (11)$$

$$P = I V \quad (12)$$

Where: I_m is current of Maximum power point, I_{ph} is strong photocurrents, I_{sc} is shunt short circuit current, I_{sh} is shunt current strength, K_1 is current strong temperature coefficient, K_v is Voltage temperature coefficient, P is PV power, R_s is PV resistance, S is solar radiation, S_{ref} is solar radiation reference (1,000 W / m²), T_{ref} is reference temperature (25⁰ C), V_m is Maximum power point voltage, V_{oc} is open-circuit voltage.

The sensor used in this study is the Light Dependent Resistor (LDR). It is used to measure the incident light to obtain the optimum angle of rotation [4, 8-9]. The relationship between the input and output of LDR can be expressed as follows:

$$\log(R) = -3/4 * \log(I_{eff} + 5) \quad (13)$$

To determine the effective light intensity value obtained over the course of one day, we can calculate it using the following formula, where I_{eff} represents the intensity of solar light, R is the electrical resistance, I_{max} is the maximum intensity value for each LDR, and θ_{eff} is the angle of incidence of solar radiation that determines the effective light intensity:

$$I_{eff} = I_{max} * \sin(\theta_{eff}) \quad (14)$$

The Linear Actuator is used to move the panels up or down and right to left [6, 32, 35]. The linear actuator is modeled mathematically as given in equation (15).

$$\frac{X(s)}{E_a(s)} = \frac{K_t}{P((J_m s^2 + D_m s)(R_a + L_a s) + K_t K_b s)} \quad (15)$$

Where: K_t is the linear motor's torque constant factor, J_m is the linear motor's moment of inertia of the rotor, D_m is the linear motor's viscous friction constant, R is electric resistance, L_a is electric inductance, K_b is electromotive force constant, P is the angular distance factor of the linear distance.

The equation (15) can be represented by state variables as follows.

$$\begin{bmatrix} \dot{x}_1 \\ \dot{x}_2 \\ \dot{x}_3 \end{bmatrix} = \begin{bmatrix} 0 & 1 & 0 \\ 0 & -\frac{D_m}{J_m} & \frac{P K_t}{J_m} \\ 0 & -\frac{k_b}{P L_a} & -\frac{R_a}{L_a} \end{bmatrix} \begin{bmatrix} x_1 \\ x_2 \\ x_3 \end{bmatrix} + \begin{bmatrix} 0 \\ 0 \\ \frac{1}{L_a} \end{bmatrix} u \quad (16)$$

$$y = [1 \quad 0 \quad 0] \begin{bmatrix} x_1 \\ x_2 \\ x_3 \end{bmatrix}$$

III. EXPERIMENTAL TEST-RIG SETUP

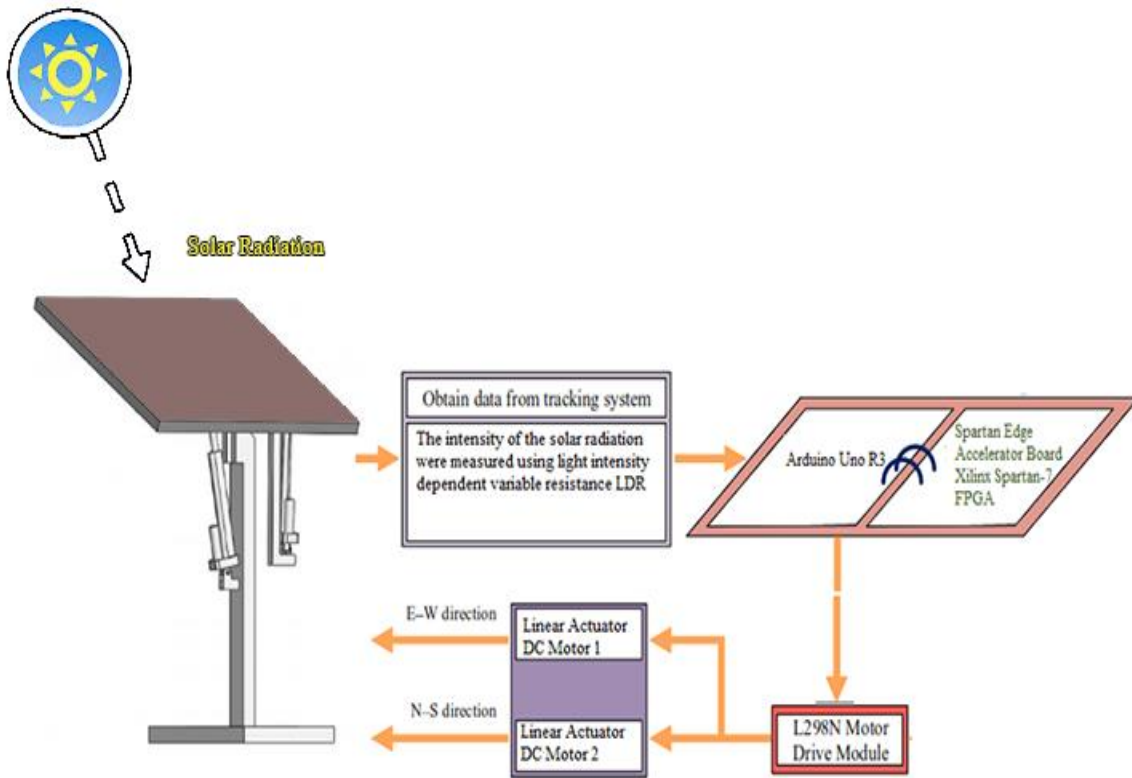
The solar test rig was investigated via two Linear motors. The selection was confirmed based on more advantages offered by the linear motor such as simplicity in design with reduced

moving parts in the motor. Besides, it can maintain operation at high speed, is self-contained, same behavior as an actuator in retracting and extending. In addition, it can produce high torque and minimum noise, and it can give an accurate rotation within restricted. The FPGA was proposed to be the control core of the system based on a certain sequence coding. EL Arish city is located in Egypt with coordinates of +31.13 (31°07'48"N), and +33.8 (33°48'00"E). Consequently, the sun's position will change substantially during the year [43].

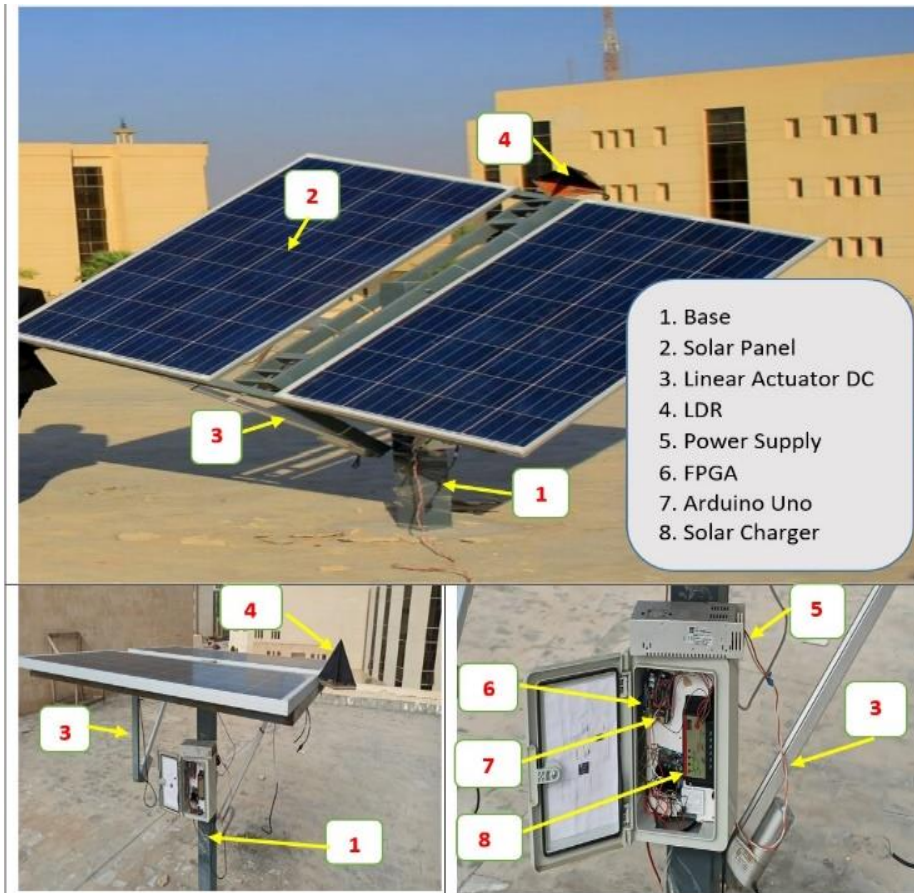
The position of the sun differs significantly during definite seasons. The input stage is designed to facilitate the conversion process of the incident light into a voltage via the light-dependent resistors (LDRs) [24]. Consequently, a comparison between the two voltages produced by LDRs in the form of error signals, is given to the microcontroller board. The generated error is used by the linear actuator to move at an angle to regulate the position of the solar panel until the error reaches zero, which means the LDR signals are equal. The LDRs error voltages are represented in analogue readings. The analogue-to-digital converter (ADC) is used to convert the analog sensor reading to integer reading values, which are compared to obtain the difference volt for the movement of the motor. This volt is given to the actuator to move to guarantee the two sensors are at equal inclination. This is known as they will give the same amount of incident light, and the panel will collect the sunlight at 90°. The sequence is repeated throughout the day [25]. The tracker systems are developed based on two principles. The two types are the normal type principle of incidence and reflection as given in this study, and the other is the type based on the working of solar (PV) panels to generate electricity. Both of these types of principles can be merged to produce approximately double the output of the panel [26].

As explained, the tracking technique is dependent on the comparison phase of coupled LDR sensors, which are mounted relatively to the axes of rotation [28]. LDR sensors 1 and 2 ($V_{E,1}$ & $V_{W,2}$, respectively) control the primary axis rotation (Zenith angle) through pitch motor 1, while sensors 3 and 4 ($V_{N,3}$ & $V_{S,4}$, respectively) are compared to control the secondary axis rotation (Azimuth angle) through yaw motor 2.

In this research, the panel of PV is utilized to generate electrical power from solar energy. The LDR is a sensor based on variation of incident solar radiation to sense the distinct position of the solar panel with the sun [28]. The motion of the panel to track the sun is created via two linear actuator DC motors. The system is supported with a solar charger to control and create safe charging for the lead acid batteries. The two motors are controlled via a module of the motor driver with the type of L298N according to the controlled signal from the FPGA board. The used type of FPGA board is Spartan Edge Accelerator Board Xilinx Spartan-7 XC7S15. The FPGA is operated simultaneously to receive and adjust the signal from LDR and make an appropriate control signal to the two motors with their encoders. Figure 3 demonstrates the flowchart operation for the sequence and conditions for the decision for the tracker system.



(b)



(a)

Fig. 2. (a). Experimental test rig for DASTS (b). Schematic diagram of experimental system

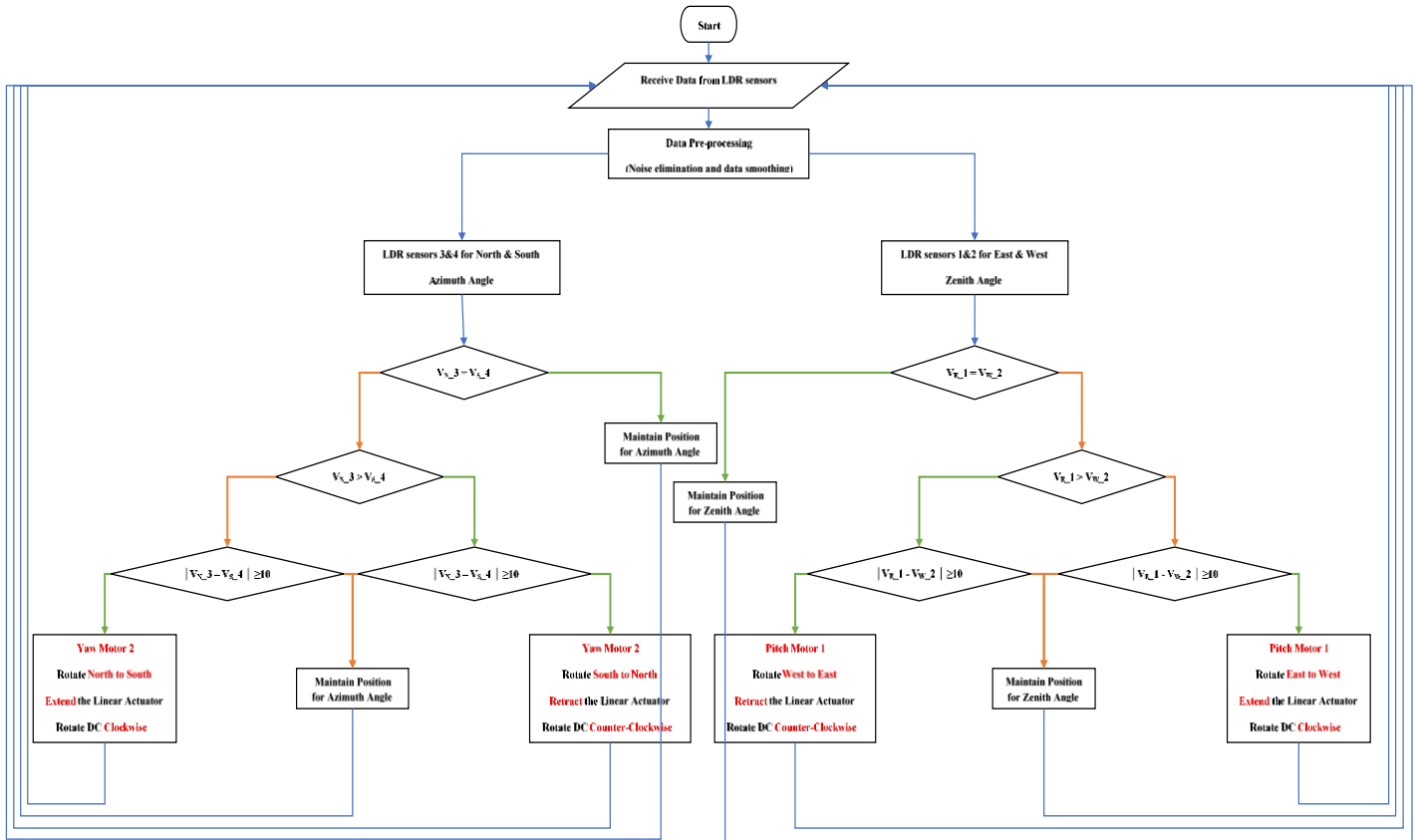


Fig. 3. Flowchart of DASTS Operation

IV. CONTROL DESIGN

MPC is one of the distinct control methods that has been widely used recently in many applications [29-31]. It is found that in this approach, the calculated control procedures are based on minimizing the cost function of the dynamic system under study and restricted to a limited and declining field. In the MPC method, it is known that this controller, at each time step, receives the system regulator or calculates the current state of the studied system. In addition, it then estimates the sequence of control procedures and decisions that reduce the cost over the horizon by finding a solution to the optimization problem, which builds on the internal mathematical model of the studied system and depends on the current state of the system [29-31]. Then the methodology applies the proposed system as the first calculated control measure only, neglecting the other following procedures. After that, this sequence is repeated in the next time step. The MPC methodology is illustrated in Figure 4.

Using the model to be controlled, the output N is anticipated at any point t in the future. The forward control signal u that was transmitted to the system and recalculated, as well as the known values of the previous input and output at time t , are what determine this output prediction. The objective function is optimized to produce the control signal u , which is often the error between the predicted output signal and the predicted reference path [29]. Based on past and current data, the model is used to forecast future system outcomes. To generate optimal input that may be utilized in the model for additional calculations, the optimization variable is stated by minimizing the objective function. The following is a prediction model for the discrete-time state space model [30, 31].

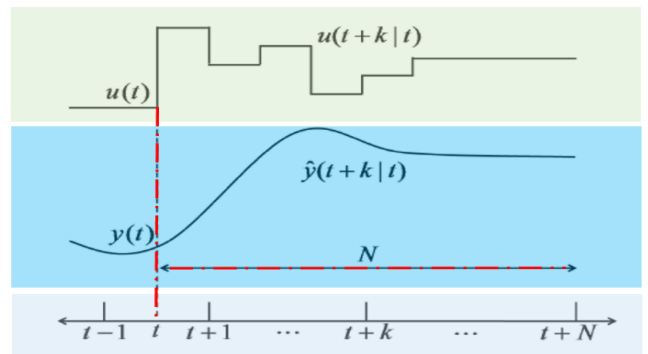


Fig. 4. MPC controller operation [28]

$$\begin{aligned} \mathbf{x}(k+1) &= \mathbf{A}_d \mathbf{x}(k) + \mathbf{B}_d \mathbf{u}(k) \\ \mathbf{y}(k+1) &= \mathbf{C} \mathbf{x}(k) \end{aligned} \quad (17)$$

$\mathbf{A}_d \in \mathbb{R}^{n \times n}$ and $\mathbf{B}_d \in \mathbb{R}^n$ are discrete time state space matrices using the exponential hold discretization method as follows:

$$\begin{aligned} \text{parent } \mathbf{A}_d(t) &= e^{A T} \\ \mathbf{B}_d(t) &= \left(\int_0^T e^{A \lambda} d\lambda \right) \mathbf{B} \end{aligned} \quad (18)$$

$$e^{A T} = I + A T + \frac{1}{2!} A^2 T^2 + \dots + \frac{1}{n!} A^n T^n + \dots \quad (19)$$

Next, the objective's function general form is deduced as the summation of the errors of the output variable y with reference y_d and the changes in the control variable u that affect it:

$$J(k) = \sum_{i=1}^P \|y(k+i/k) - y_d(i)\|_{Q_i}^2 + \sum_{j=1}^M \|u(k+j-1/k)\|_{R_j}^2 \quad (20)$$

Where P is the prediction in the time domain, M is the control in the time domain, Q and R are the weight coefficients where $Q > 0$ and $R > 0$ or in the form of a symmetric positive definite matrix.

The MPC problem can be solved as an optimization problem by minimizing the objective function J and the constraints x , y , and u :

$$\begin{aligned} \text{Min } U(k) \quad & J(k) \\ x(k+1) &= A_d x(k) + B_d u(k) \\ y(k+1) &= C_d x(k) + D_d u(k) \\ u_{\min} &\leq u(k+j-1/k) \leq u_{\max} \\ x_{\min} &\leq x(k+i/k) \leq x_{\max} \\ & i = 1, \dots, P \\ & j = 1, \dots, M \end{aligned} \quad (21)$$

Where $U(k) = [u(k), u(k+1), \dots, u(k+M-1)]^T$ is the control sequence, $\{u_{\min}, u_{\max}\}$ and $\{x_{\min}, x_{\max}\}$ are the control and state variable constraints. The proposed control configuration for the tracker based on MPC controller is given in Figure 5.

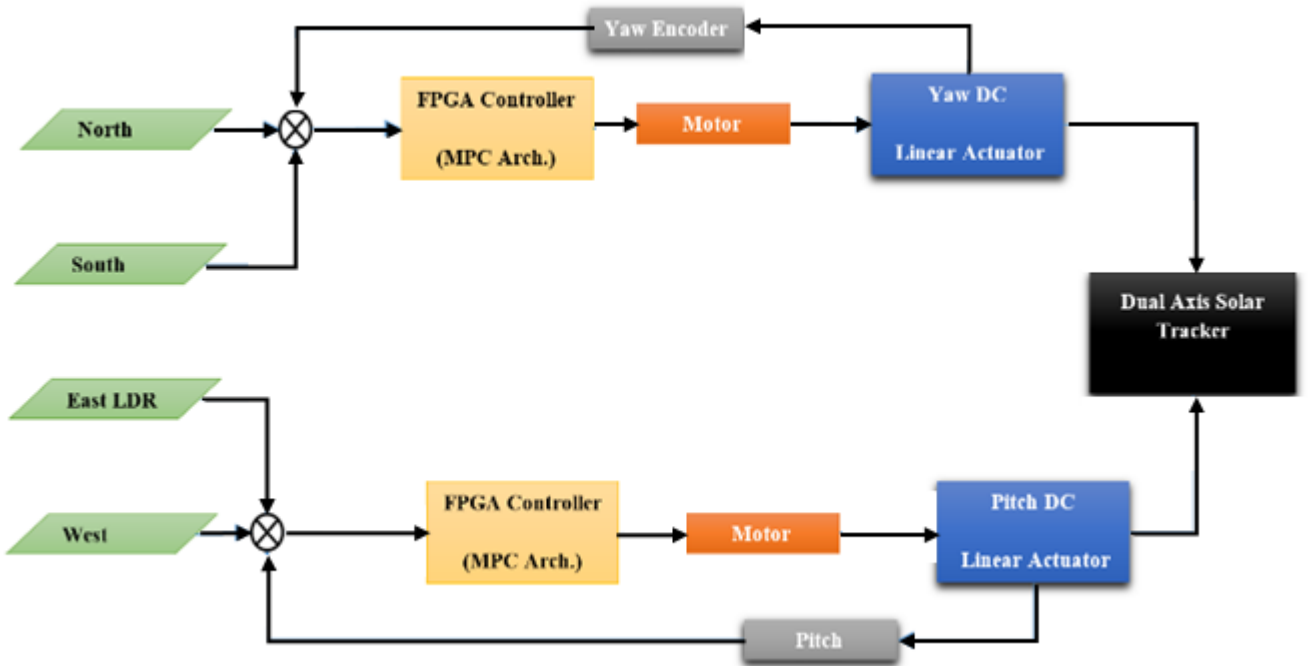


Fig. 5. Block diagram of solar system with MPC

V. IOT-BASED MONITORING SYSTEM DESIGN

The technology of IoT is widely used nowadays in different applications (see Figure 6) [38]. Implementing an IoT-based monitoring system involves integrating sensor data collection, communication protocols, and remote monitoring capabilities into the existing FPGA-based control system. This system aims to optimize solar tracking mechanisms and enhance energy harvesting efficiency [39]. The position sensors are utilized to accurately determine the position of the sun (LDRs) and the orientation of the solar panels (Linear

motors Encoders). This information is crucial for real-time adjustment of the solar tracking system. Besides, IoT connectivity module is applied to integrate IoT modules ESP8266 with the FPGA Spartan Edge Accelerator Board Xilinx Spartan-7 XC7S15 via Arduino Uno Rev3 to enable communication with external networks and devices for remote monitoring and control [40]. For the communication infrastructure, the wireless connectivity utilizes protocols such as Wi-Fi for wireless communication between the FPGA-based control system and external devices. The process of internet connectivity enables the system to connect

to the internet for remote monitoring and data transmission to cloud platforms or monitoring servers [41]. In case of monitoring and control based on IoT, platform of web interface is developing for user-friendly interface accessible through web browsers. This interface allows users to monitor system performance, adjust settings, and receive real-time notifications. Furthermore, there are data visualization technologies that are employed to visually represent sensor data, control outputs, and energy generation parameters. Graphical representations are effective in aiding users' comprehension of system behavior and performance patterns. The Internet of Things (IoT) offers various benefits, including enhanced efficiency, system monitoring and control, decision-making capabilities, and adaptability and scalability [42].

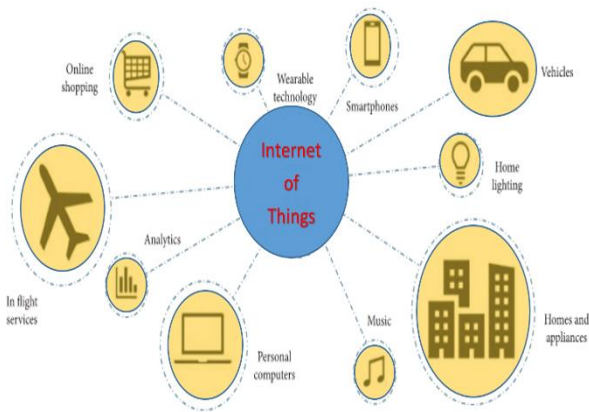


Fig. 6. Applications of IoT

VI. RESULTS

The experimental test rig of the dual-axis solar tracker system (DASTS) is built and tested to prove the performance of the tracker system and evaluate the control system design. The experimental study is tested in Al-Arish City, Sinai University on 09 Nov. implementing PID, 13 Nov. implementing FOPID and 17 Nov. implementing MPC, Egypt. In this research, the results of different control strategies are compared to fixed-panel solar systems. We suggested PID, FOPID, and MPC to control the experimental system. The study juxtaposed the outcomes of these varied control methodologies against those of fixed-panel solar systems. For the fixed panel system and solar tracker system-based control approaches, the open voltage (V_{oc}), short circuit current (I_{sc}), generated power (P), and irradiation (G) are measured in numerical values and graphs. The measurements of chosen parameters are taken in a period from 8:20 AM to 4:22 PM.

The generated voltages, currents, power, and irradiation-based PID and fixed system are shown in Table 1. Table 2 presents the experimental results of FOPID and fixed system. Moreover, the DASTS-based MPC is compared with the fixed system in Table 3. The measurements were collected on four different days. The measurements of voltage, currents, irradiance, and power for fixed PV systems for different four days based on control strategies are given in Figures 7-10. In addition, the measurements of the fixed PV system are carried out with an angle of panel about 31.13 degrees. Figure 7

demonstrates the open circuit voltage for a fixed PV system. The short circuit current measurement for fixed solar is presented in Figure 8. Besides, the generated power of the fixed panel is shown in Figure 9. Figure 10 displays the measurements of irradiance of solar in the case of a fixed panel. Considering, the plotted data in Figures 7-10 and numerical values in Tables 1-3, the results show that the fixed data are very close to each other for four different days.

The obtained data prove that the comparison between the fixed solar PV system and the tracker system based on different controllers will be in a close environment and very fair. We plotted the comparison between the response of PID, FOPID, and MPC for the open circuit voltage of the tracker DASTA system in Figure 11. The waveform of output voltage-based MPC is higher than the other controllers as shown in Figure 11. The short circuit current-based tracker system is given in Figure 12. From this figure, the measurement of short circuit current-based MPC is greater than other control strategies. The generated power for the tracker DASTA PV system is shown in Figure 13. The collected data of power are measured in case of applying suggested controllers. The tracker-based MPC controller shows a high generated power in comparison with the suggested controllers (see Figure 13). In addition to the obtained results, the waveform of irradiance of solar is displayed in Figure 14.

Gain of energy is, as is well known, the most important consideration when evaluating the tracker system. The energy gain is the amount that the suggested tracking system increases generated energy in comparison to the fixed panel system. On the other hand, the energy consumption of the linear actuator must be taken into account to determine the net gain in energy for the tracking DASTS. However, in this research, we neglected this consumption due to external supply for the actuators. As shown in Tables (1-3), the performance of the DASTS was significantly low at noon. The average production of energies for the fixed and DASTS based on the PID controller was 143.11 W.h and 168.9 W.h, respectively. Consequently, an additional yield of $(168.9-143.11)/143.11 = 0.1801$ or 18.01 % energy generation was obtained. In addition, the average generation for fixed and DASTS based on FOPID were 146.12 W-h and 172.46 W-h respectively, this demonstrates an increase in production of 18.03%. In the same context, the generation in fixed and DASTS based on MPC are 149.04 W-h and 179.2 W-h respectively. The additional production is about 20.26 %. Based on the increase of generated energy from fixed and DASTS, the improved electricity production is much enhanced in the case of DASTS-based MPC with 20.26% compared with 18.01% and 18.03 % for DASTS-based PID and FOPID respectively.

In conclusion, the findings underscore the pivotal role of control strategies in optimizing energy generation within solar tracking systems. The discerned performance differentials highlight the efficacy of MPC-based control in maximizing energy output, thus advocating for its adoption in solar energy systems to enhance overall efficiency and sustainability.

TABLE 1. MEASUREMENTS OF EXPERIMENTAL PARAMETERS-BASED TRACKER WITH PID AND FIXED SYSTEM

Hours	V _{oc}		I _{sc}		P=VI		G	
	Fixed	PID	Fixed	PID	Fixed	PID	Fixed	PID
8:20	20.1	20.3	7.2	7.7	143.9	155.9	850	1090
9:32	20.2	20.3	7.2	7.8	146	158.9	865	1093
10:36	20.2	20.4	8.1	8.9	164.2	180.4	989	1097
11:27	20.3	20.5	8.8	8.9	177.5	183.1	1059	1110
12:01	20.4	20.5	8.9	8.9	181.2	184.1	1088	1111
12:44	20.2	20.4	8.7	8.9	176.7	181.8	1064	1105
13:28	20.1	20.2	8.1	8.9	163.6	179.8	976	1102
14:36	20	20.1	6.8	8.7	136	175.3	815	1085
15:45	19.8	20	4.9	8.4	96.8	167.6	572	1025
16:22	19.3	19.6	3.6	6.2	69.5	122.3	335	822

TABLE 2. MEASUREMENTS OF EXPERIMENTAL PARAMETERS-BASED TRACKER WITH FOPID AND FIXED SYSTEM

Hours	V _{oc}		I _{sc}		P=VI		G	
	Fixed	FOPID	Fixed	FOPID	Fixed	FOPID	Fixed	FOPID
8:20	20.3	20.5	7.2	7.8	147	159	800	1080
9:32	20.4	20.5	7.3	7.9	149	162	855	1083
10:36	20.4	20.6	8.2	9	168	184	970	1087
11:27	20.5	20.7	8.8	9	181	187	1049	1100
12:01	20.6	20.7	8.9	9.1	185	188	1078	1101
12:44	20.4	20.5	8.8	9	180	185	1054	1095
13:28	20.3	20.4	8.2	8.9	167	184	966	1092
14:36	20.2	20.3	6.9	8.8	139	179	805	1075
15:45	20	20.2	4.9	8.5	99	171	562	1015
16:22	19.5	19.8	3.6	6.4	71	127	325	812

TABLE 3. MEASUREMENTS OF EXPERIMENTAL PARAMETERS-BASED TRACKER WITH MPC AND FIXED SYSTEM

Hours	V _{oc}		I _{sc}		P=VI		G	
	Fixed	MPC	Fixed	MPC	Fixed	MPC	Fixed	MPC
8:20	20.5	20.7	7.3	8	149.9	165.6	870	1110
9:32	20.6	20.8	7.4	8.5	152	176.4	885	1113
10:36	20.6	20.8	8.3	9	171	187.9	1009	1117
11:27	20.7	20.9	8.9	9.1	184.8	190.5	1079	1130
12:01	20.8	20.9	9.1	9.2	188.6	191.5	1108	1131
12:44	20.6	20.9	8.9	9.1	184	189.8	1084	1125
13:28	20.5	20.8	8.3	9.1	170	188.6	996	1122
14:36	20.4	20.7	6.9	8.9	141.6	183.8	835	1105
15:45	20.2	20.5	5	8.7	100.8	178.4	592	1045
16:22	19.6	20	3.7	7	72.5	140	355	842

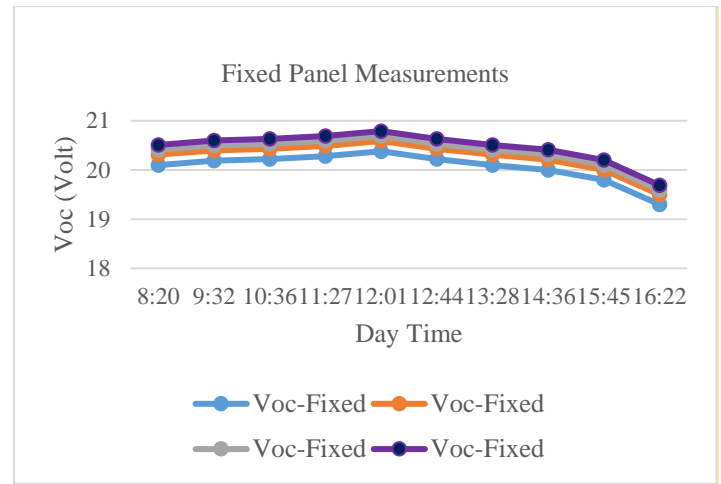


Fig. 7. Measured open circuit output voltage for fixed PV system.

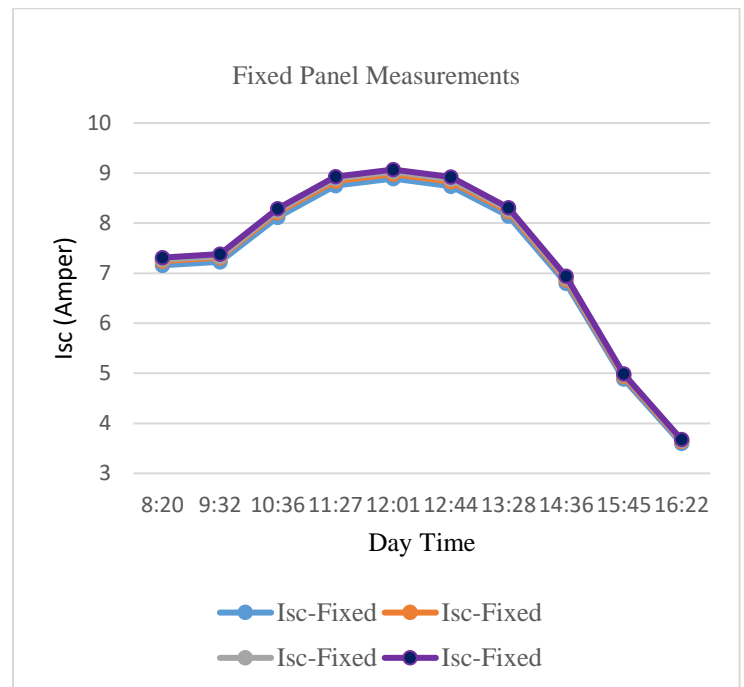


Fig. 8. Measured short circuit current for fixed PV system.

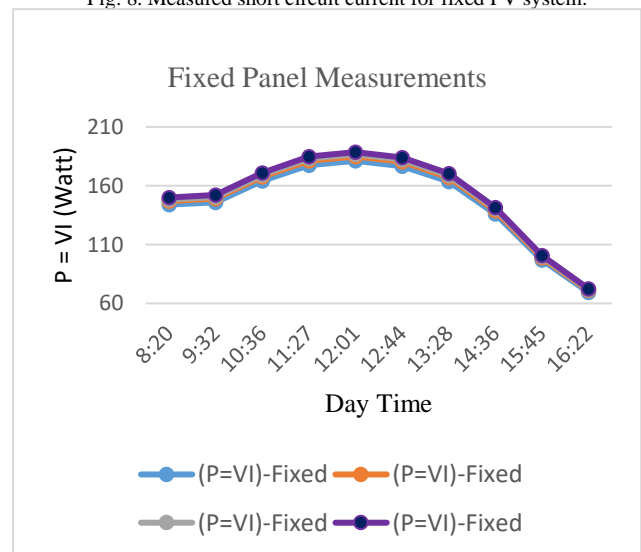


Fig. 9. Measured generation power for fixed PV system.

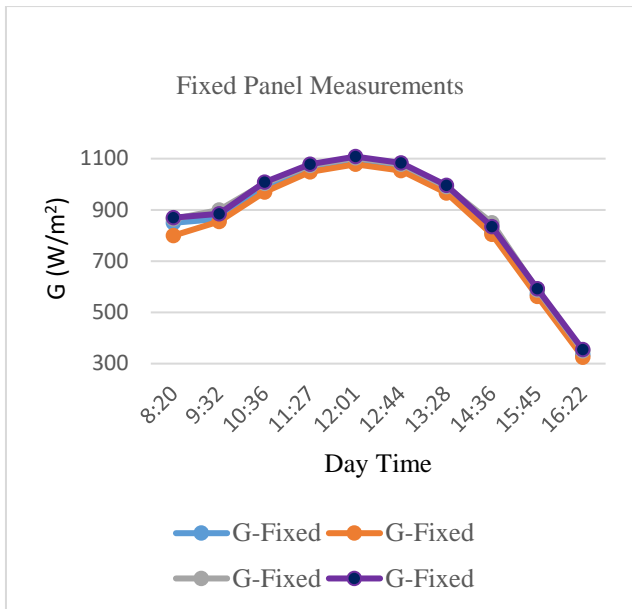


Fig. 10. Measured solar irradiation for fixed PV systems.

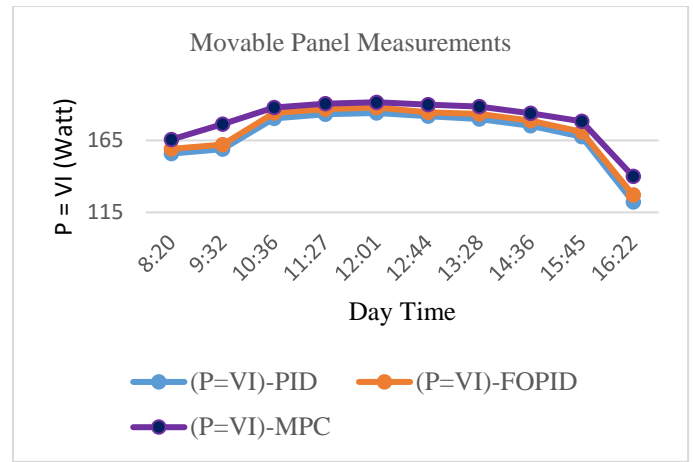


Fig.13. Measured generation power for tracker PV system.

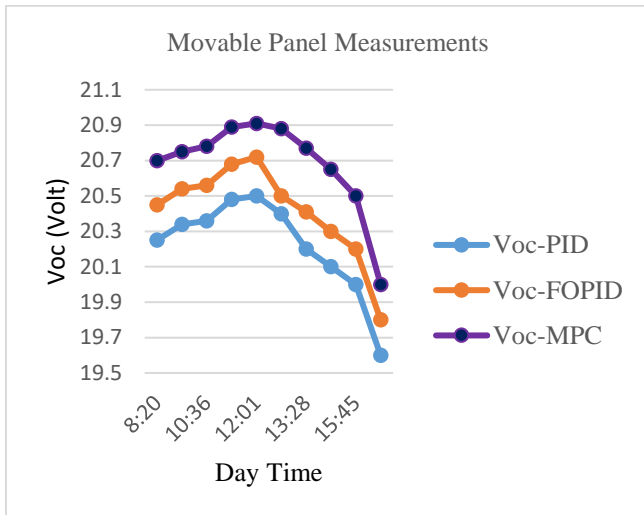


Fig. 11. Measured open circuit output voltage for tracker PV system.

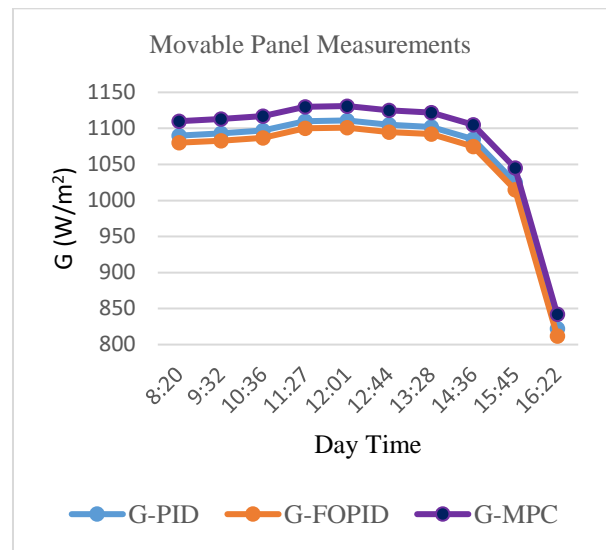


Fig. 14. Measured solar irradiation for tracker PV system.

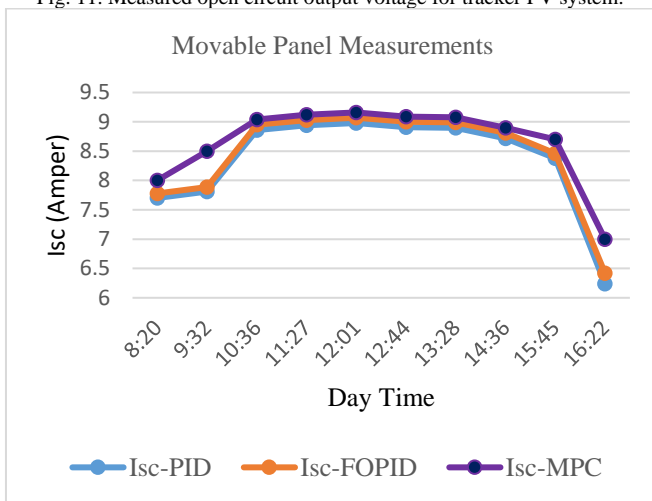


Fig. 12. Measured short circuit current for tracker PV system.

The primary purpose of applying the IoT in this research to the dual axis tracker is to facilitate the monitoring of the power generated by comparing the fixed and mobile system of solar panels, as well as controlling the stopping and running of the system (see Figures 15-18). In addition, monitoring the generated power is done through the modern technology of the IoT, which plays an important and effective role in the Industry 4.0. In this research, readings of the power are obtained in real time, which relates to the output of fixed and movable solar panels (see Figures 16-17). Figure 15 demonstrates the online link for Thingspeak IoT platform. Besides, the comparison study between generated power for fixed panels and suggested trackers using PID, FOPID and MPC are shown in Figures 16 & 17. Finally, Figure 18 presents the overview IoT Thingspeak platform with different power fields. This is done through the Thingspeak platform, which can be accessed via Wi-F and the power output of both systems will be displayed. ThingSpeak is an open service provided by MATLAB as an IoT analytics platform that helps to directly collect and analyze data streams by visualizing them in the cloud. In addition, readings can be sent to ThingSpeak from supporting devices, providing a quick visualization of the given data, and sending the necessary alerts. Obviously, from the given figures, it is found that the proposed movable solar tracking systems generate higher electricity than their fixed counterparts due to increased direct

exposure to solar rays by tracking the movement of the sun (see Figure 16-17).

The estimation of the total latency for the IoT system is carried out based the summation of delay time in sensors, FPGA, actuator and communication. The total latency could be calculated as follows.

$$\text{Total Latency} = 2 \text{ ms (sensor)} + 1 \mu\text{s (FPGA)} + 200 \text{ ms (actuator)} + 10 \text{ ms (communication)}$$

$$\text{Total Latency} = 2 \text{ ms} + 0.001 \text{ ms} + 200 \text{ ms} + 10 \text{ ms} = 212.001 \text{ ms}$$

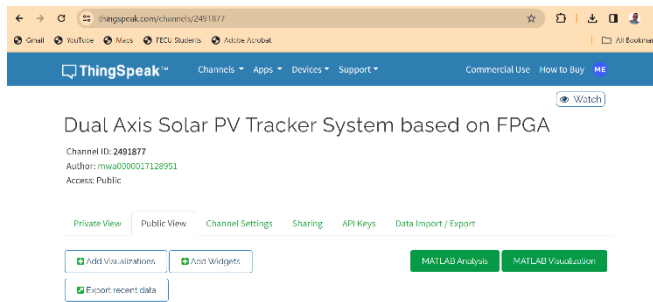


Fig. 15. Thingspeak IoT platform for the DAST system.

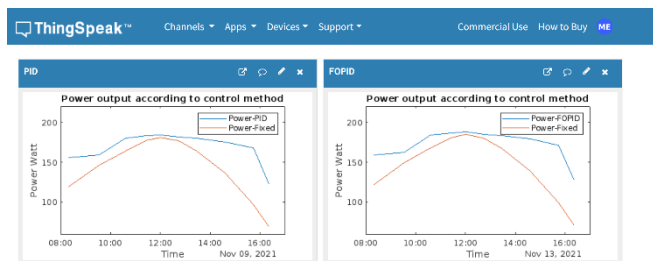


Fig. 16. Published generated power on Thingspeak IoT platform based PID and FOPID

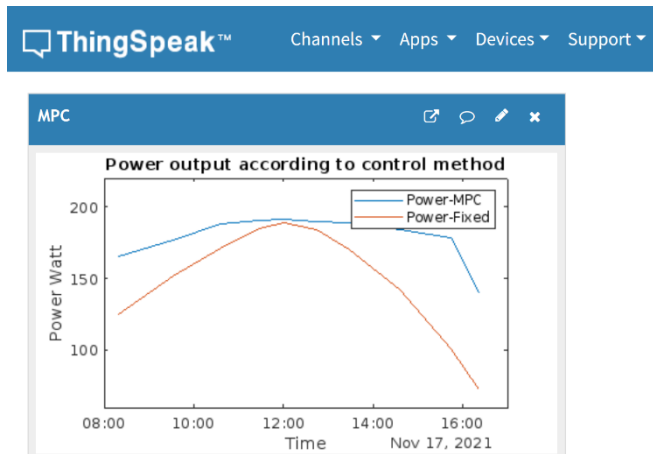


Fig. 17. Published generated power on Thingspeak IoT platform based on MPC

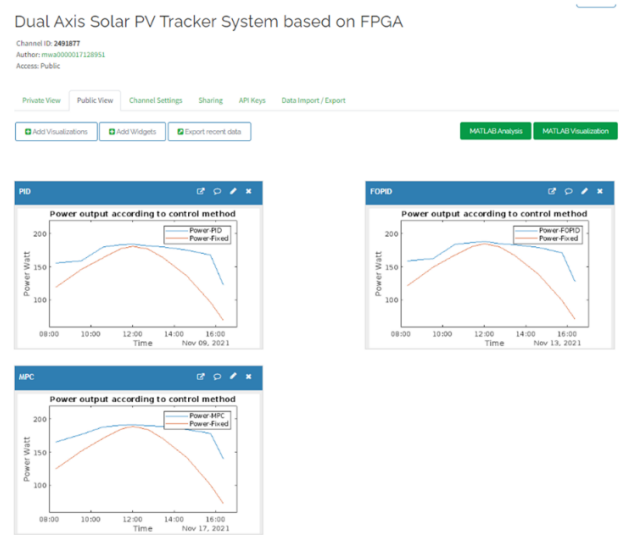


Fig. 18. Overview for the IoT platform with different fields

VII. CONCLUSIONS

The presented research has discussed a simple, novel control investigation of a sun-tracking system that uses a dual-axis system based on two linear actuators to track the sun. The MPC controller is proposed to improve the efficiency of the DASTA system, and it is compared to the PID and FOPID controllers. The FPGA is utilized as the core of the control system implementation to receive the signals from sensors and send the control signal to the actuators. An experimental prototype laboratory has been effectively constructed and tested to prove the effectiveness of the proposed control strategy. The experiment results showed that the established system of DASTA based on MPC increased the amount of energy up to 20.2% for a 300 W PV system. The proposed strategy is considered an effective approach for improving the generation of solar systems. It provides some good-looking features such as the capability to move the two axes of the system within different ranges, modify the accuracy of tracking, have more advantages based on using FPGA, and control investigation with cost-effectiveness. Finally, the experimental results lead us to trust that, this work offers some scientific contributions to the improvement of applications of solar energy based on MPC controllers and FPGAs.

ACKNOWLEDGMENT

The authors would like to extend their sincere thanks and appreciation to the Academy of Scientific Research and Technology (ASRT), Cairo, Egypt, for their assistance, advice, and provision of the components required to complete this research.

VIII. REFERENCES

- [1] "World Energy Outlook 2024," OECD, 2024. [Online]. Available: <https://doi.org/10.1787/557a761b-en>. [Accessed: 30-May-2024].
- [2] "Energy Outlook 2024 Edition," BP, 2024. [Online]. Available: <https://www.bp.com/en/global/corporate/energy-economics/energy-outlook.html>. [Accessed: 30-May-2024].

- [3] "IRENA, Renewable capacity statistics 2024," 2024. [Online]. Available: <https://www.irena.org/publications/2020/Mar/Renewable-Capacity-Statistics-2020>. [Accessed: 30-May-2024].
- [4] EIA, "Post covid-19, further reform is necessary to accelerate china's clean energy future," 2024. [Online]. Available: <https://www.iea.org/articles/post-covid-19-further-reform-is-necessary-to-accelerate-china-s-clean-energy-future>. [Accessed: 30-May-2024].
- [5] EIA, "Sustainable recovery," 2024. [Online]. Available: <https://www.iea.org/reports/sustainable-recovery>. [Accessed: 30-May-2024].
- [6] EIA, "International energy outlook 2024," 2024. [Online]. Available: <https://www.eia.gov/outlooks/ieo/>. [Accessed: 30-May-2024].
- [7] J. Li and J. Huang, "The expansion of China's solar energy: Challenges and policy options," *Renew. Sustain. Energy Rev.*, vol. 132, p. 110002, 2020.
- [8] Y. Heng, C.-L. Lu, L. Yu, and Z. Gao, "The heterogeneous preferences for solar energy policies among US households," *Energy Policy*, vol. 137, p. 111187, 2020.
- [9] L. Cheng et al., "Solar energy potential of urban buildings in 10 cities of China," *Energy*, vol. 196, p. 11703, 2020.
- [10] M. Fan, H. Cheng, and Z. Wu, "Optimized energy storage system configuration for voltage regulation of distribution network with PV access," in *2023 IEEE Sustainable Power and Energy Conference (ISPEC)*, IEEE, 2023, doi: 10.1109/ISPEC.2023.10132567.
- [11] Y. Zhang, H. Liu, and X. Tian, "Optimal Allocation of Hybrid Energy Storage System Based on Smoothing Wind Power Fluctuation and Improved Scenario Clustering Algorithm," *Processes*, vol. 11, no. 12, pp. 3407, Dec. 2023, doi: 10.3390/pr11123407.
- [12] A. P. Gonzalo, A. P. Marugán, and F. P. G. Márquez, "Survey of maintenance management for photovoltaic power systems," *Renew. Sustain. Energy Rev.*, vol. 134, p. 110347, 2020.
- [13] P. Ochoa et al., "Modeling and experimental validation and thermal performance assessment of a sun-tracked and cooled PVT system under low solar irradiation," *Energy Convers. Manage.*, vol. 222, p. 113289, 2020.
- [14] C. Alexandru, "Optimization of the bi-axial tracking system for a photovoltaic platform," *Energies*, vol. 14, p. 535, 2021.
- [15] C. Alexandru, "Simulation and Optimization of a Dual-Axis Solar Tracking Mechanism," *Mathematics*, vol. 12, no. 7, p. 1034, 2024. doi: 10.3390/math12071034.
- [16] M. Alanazi et al., "A Comprehensive Study on the Performance of Various Tracker Systems in Hybrid Renewable Energy Systems, Saudi Arabia," *Sustainability*, vol. 15, no. 13, p. 7598, July 2023, doi: 10.3390/su15137598.
- [17] M. R. Setiawan, A. D. Sutanto, and E. Y. Syamsuddin, "A Comprehensive Review of Solar Tracking Systems: Technologies, Applications, and Future Trends," *International Journal of Renewable Energy Research*, vol. 13, no. 2, pp. 759-782, 2023, doi: 10.20508/ijrer.v13i2.16950.
- [18] S. Seme et al., "Solar photovoltaic tracking systems for electricity generation: A review," *Energies*, vol. 13, p. 4224, 2020.
- [19] I. A. Badruddin, T. M. Yunus Khan, and E. Jassim, "Harnessing Solar Power: A Review of Photovoltaic Innovations, Solar Thermal Systems, and the Dawn of Energy Storage Solutions," *Energies*, vol. 16, no. 18, p. 6456, Sep. 2023, doi: 10.3390/en16186456.
- [20] A. Awasthi et al., "Review on sun tracking technology in solar PV system," *Energy Rep.*, vol. 6, pp. 392-405, 2020.
- [21] Y. Zhu, J. Liu, and X. Yang, "Design and performance analysis of a solar tracking system with a novel single-axis tracking structure to maximize energy collection," *Appl. Energy*, vol. 264, p. 114647, 2020.
- [22] N. Kuttybay et al., "Optimized single-axis schedule solar tracker in different weather conditions," *Energies*, vol. 13, p. 5226, 2020.
- [23] I. K. AlMadani, A. M. Almahdi, and S. Ali, "Experimental Investigation of Azimuth- and Sensor-Based Control Strategies for a PV Solar Tracking Application," *Applied Sciences*, vol. 12, no. 9, p. 4758, 2022, doi: 10.3390/app12094758
- [24] R. Gupta et al., "Enhanced control algorithm for maximizing energy extraction in two-axis solar PV tracking systems," *Solar Energy*, vol. 188, pp. 305-315, 2022.
- [25] H. Zhang et al., "Optimization of solar panel tracking control using adaptive type-2 fuzzy sliding mode control," *IEEE Transactions on Industrial Electronics*, vol. 69, no. 7, pp. 5956-5965, 2022.
- [26] A. Kumar et al., "Optimization of Type-2 Fuzzy Sliding Mode Control for Mobile Inverted Pendulum Systems using Genetic Algorithm," *IEEE Transactions on Industrial Electronics*, vol. 68, no. 9, pp. 8176-8185, 2021.
- [27] A. K. Devarakonda et al., "A comparative analysis of maximum power point techniques for solar photovoltaic systems," *Energies*, vol. 15, no. 22, p. 8776, 2022.
- [28] A. Patel, S. Gupta, and R. Sharma, "Real-time implementation of model predictive control for dual-axis solar tracker using FPGA," in *2022 IEEE International Conference on Renewable Energy Integration into Smart Grids (REISG)*, 2022, pp. 120-125.
- [29] Y. Hu, Y. Liu, and Z. Liu, "A survey on convolutional neural network accelerators: GPU, FPGA and ASIC," in *2022 14th International Conference on Computer Research and Development (ICCRD)*, 2022, pp. 100-107.
- [30] P. Babu and E. Parthasarathy, "Reconfigurable FPGA architectures: A survey and applications," *Journal of The Institution of Engineers (India): Series B*, vol. 102, no. 2, pp. 143-156, 2021.
- [31] A. Sidek and M. M. Som, "A Review of FPGA-based Implementation related to Electrical Engineering and Contribution to MPPT, Converter and Motor Drive Control," *Multidisciplinary Applied Research and Innovation*, vol. 2, no. 1, pp. 357-365, 2021.
- [32] L. Bustio-Martínez et al., "FPGA/GPU-based acceleration for frequent itemsets mining: A comprehensive review," *ACM Computing Surveys (CSUR)*, vol. 54, no. 9, pp. 1-35, 2021.
- [33] P. Krupa, D. Limon, and T. Alamo, "Implementation of model predictive control in programmable logic controllers," *IEEE Transactions on Control Systems Technology*, vol. 29, no. 3, pp. 1117-1130, 2020.
- [34] V. Patne, D. Ingole, and D. Sonawane, "FPGA implementation framework for low latency nonlinear model predictive control," *IFAC-PapersOnLine*, vol. 53, no. 2, pp. 7020-7025, 2020.
- [35] P. Krupa, D. Limon, and T. Alamo, "Implementation of model predictive control in programmable logic controllers," *IEEE Transactions on Control Systems Technology*, vol. 29, no. 3, pp. 1117-1130, 2020.
- [36] B. Wang, J. Jiao, and Z. Xue, "Implementation of Continuous Control Set Model Predictive Control Method for PMSM on FPGA," *IEEE Access*, vol. 11, pp. 12414-12425, 2023.
- [37] A. Almutairi and F. Alzahrani, "Design and Implementation of a Dual-Axis Solar Tracking System Using an FPGA," *IEEE Access*, vol. 9, pp. 57968-57978, 2021.
- [38] S. Banerjee, P. De, and A. Chakrabarti, "IoT-Based Solar Tracking System with FPGA Implementation," *IEEE Sensors Journal*, vol. 20, no. 15, pp. 8249-8257, 2020.
- [39] R. Manandhar and R. K. Manandhar, "FPGA Implementation of Solar Tracking System with IoT Enabled Monitoring System," in *2021 1st International Conference on Renewable Energy and Green Technology (ICREGT)*, 2021, pp. 1-4.
- [40] A. Sharma and H. Patel, "IoT-Based Solar Tracking System with FPGA Implementation," *International Journal of Advanced Engineering Research and Science*, vol. 8, no. 2, pp. 237-244, 2021.
- [41] W. Sun and Y. Huang, "FPGA-Based Solar Tracking System with IoT Connectivity," in *2021 9th International Conference on Smart Grid and Clean Energy Technologies (ICSGCE)*, 2021, pp. 51-56.
- [42] W. Sun and Y. Huang, "FPGA-Based Solar Tracking System with IoT Connectivity," in *2021 9th International Conference on Smart Grid and Clean Energy Technologies (ICSGCE)*, 2021, pp. 51-56.
- [43] A. Elshinawy, et al., "Evaluation of solar radiation resources in North Sinai region, Egypt," *Solar Energy*, vol. 150, pp. 321-335, 2023. doi: 10.1016/j.solener.2022.12.001.